Short Communication

Aligned carbon nanotube/polymer composite film with anisotropic tribological behavior

Hui Zhang, Longbin Qiu, Houpu Li, Zhitao Zhang, Zhibin Yang, Huisheng Peng *

State Key Laboratory of Molecular Engineering of Polymers, Department of Macromolecular Science, and Laboratory of Advanced Materials, Fudan University, Shanghai 200438, China

ABSTRACT

A general method had been developed to prepare highly aligned carbon nanotube/polymer composite films, which represented the first composite material with an anisotropic tribological property on the surface. The friction coefficient in the transverse direction was about 2 times of that of longitudinal direction. In addition, the aligned nanotubes provided the composite film with excellent electrical, mechanical, and thermal properties. This work also presented an efficient paradigm to synthesize friction materials with an anisotropic tribological behavior by introduction of one-dimensional nanostructures.

© 2012 Elsevier Inc. All rights reserved.

1. Introduction

Due to the low cost, easy fabrication, tunable structure, and high performance, polymers had been widely studied and used for friction materials [1–3]. To further improve the tribological property, a second phase such as Kevlar, metal oxide, nonmetal oxide, and nonmetal, was usually introduced to form composite materials with incorporated new properties [4–7]. To this end, it was critically important to design and prepare such composite materials at nanoscale as the structure could be more accurately controlled, and the property may be more efficiently improved [8,9]. Although a wide variety of nanocomposites had been investigated, the resulting materials were mainly isotropic in both structure and tribological property. However, in many applications such as aerospace crafts, automobiles, and ships, both anisotropic structures and tribological behaviors were highly required but remain challenging [10,11]. Generally, a nonsymmetrical structure may be realized by introducing Janus nanoparticles or one-dimensional nanostructures including nanotubes, nanorods, and nanowires [12–15], though such designs were rare in the preparation of friction materials.

Carbon nanotubes (CNTs) represented one of the most studied one-dimensional nanostructures [13]. They were typically considered as molecular-scale tubes of graphitic carbon. The unique structure provided CNTs with extraordinary electrical, mechanical, and thermal properties. For instance, CNTs can be metallic or semiconducting depending on their structures, and the electrical conductivity was on the level of 10^5 S/cm [16]. The Young's modulus of CNTs can be as high as 1000 GPa (approximately 5 times higher than steel), and the tensile strength may achieve 100 GPa (around 100 times higher than steel) [17,18]. CNTs also showed a high thermal conductivity of 6000 W/(m K), compared with 371 and 40.8 W/(m K) for copper and steel, respectively [19]. Due to the combined excellent properties, CNTs had been proposed for a broad spectrum of applications in the fields of materials, electronics, field emission, biology, medicine, and electrochemistry [20–23]. In many cases, CNTs were incorporated into polymers to combine the excellent properties of CNT and polymer and even brought some new properties which could not be found in the individual component [20]. Three main fabrication methods had been developed to synthesize CNT/polymer composites, that is, solution blending, melt blending, and in situ polymerization [24]. However, there remained a common and critical challenge, that is, random dispersion of CNTs in polymer matrices. As a result, the composites had not fully taken advantage of the excellent properties of individual CNTs. For instance, the tensile strength and electrical conductivity of the CNT/polymer material were typically 10^1 to 10^2 MPa and 10^{-6} to 10^{-3} S/cm, respectively [25]. These limitations had largely hindered their practical applications.

Herein, highly aligned multiwalled carbon nanotube (MWCNT)/polymer composite materials had been prepared from MWCNT sheets which could be spun from MWCNT arrays. The high alignment of MWCNTs enabled excellent electrical, mechanical, and thermal properties. In particular, the side walls of aligned MWCNTs were designed to be exposed on the composite surface and represented an ideal model to study the anisotropic tribological behavior (Fig. 1 and Fig. S1). It had been found that the friction coefficient

* Corresponding author.
 E-mail address: penghs@fudan.edu.cn (H. Peng).
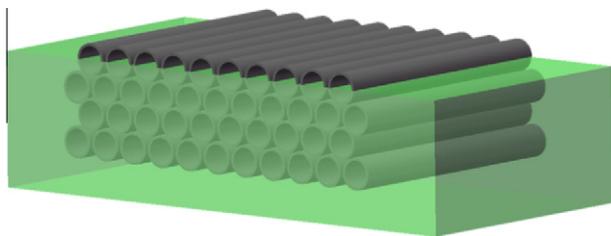
Fig. 1. Schematic illustration to the surface of aligned MWCNT/polymer composite films.

in the transverse direction was typically 2 times of that in the longitudinal direction relative to the MWCNT length.

2. Experimental section

2.1. Preparation of aligned MWCNT/PMMA composite films

The preparation of aligned MWCNT/PMMA composite films was schematically shown in Fig. S1. Spinnable MWCNT array was firstly grown on silicon substrates by a catalytic chemical vapor deposition (CVD) method [26–29]. The aligned MWCNT sheets were then pulled out of the array and closely attached onto the glass substrate. The PMMA solution in acetone (concentration of 10 wt%) was finally coated onto the MWCNT sheet, followed by evaporation of the solvent. In order to realize that the side walls of aligned MWCNTs were exposed on the film surface, it was important to make the MWCNTs be tightly contacted with the substrate. For the control experiment, randomly dispersed MWCNT/PMMA composite films were fabricated in a similar way. The as-synthesized composite films could be easily peeled off in a dilute NaOH solution. All measurements were made on the surface which was originally attached to the glass substrate.

2.2. Characterization

The structure was characterized by scanning electron microscopy (Hitachi FE-SEM S-4800, operated at 1 kV) and atomic force microscopy (SHIMADZ SPM 9500J3). For the mechanical measurements, the composite film was cut into strips and mounted on a paper tap with the gauge length of 10 mm and tested on an HY0350 Table-top Universal Testing Instrument. Electrical measurements were conducted by a two-probe method. Micro-tribological tests of the film were investigated using a friction force microscopy (DI Nanoscope IIIa FFM) under a contact mode. The probe was obtained from Appnano and mainly composed of a cantilever with a silica bead (diameter of 15 μm) at the tip. The elastic modulus and resonance frequency were 3.0 N/m and 62 kHz, respectively. All tests were carried out at room temperature and under a relative humidity of 40%. The friction signals were obtained by scanning the composite film with a constant frequency of 1.96 Hz under an external load being ranged from 0 to 100 nN. The typical track length was 5 μm. Both longitudinal and transverse directions relative to the MWCNT length were measured.

3. Results and discussion

Spinnable MWCNT arrays were synthesized by a typical chemical vapor deposition process according to our previous reports [30]. Specifically, Fe (1.2 nm)/Al$_2$O$_3$ (3 nm) deposited on silicon wafer was used as the catalyst, ethylene as the carbon source, and a mixture of argon and hydrogen as the carrying gas. The growth of MWCNT array was performed at 750 °C for 10 min.

Fig. 2a showed scanning electron microscopy (SEM) image of a representative spinnable MWCNT array with a height of about 250 μm. The resulting MWCNTs exhibited a multi-walled structure with a diameter of about 10 nm (Fig. S2). Uniform MWCNT sheets with lengths of tens of meters could be then continuously pulled out of the array, and the MWCNTs were aligned along the drawing direction. Fig. 2b showed the SEM image of a typical MWCNT sheet in which MWCNTs were highly aligned. The size of voids among neighboring nanotubes was ranged from 50 to 200 nm. A series of MWCNT sheets could be further stacked along the same direction to produce thicker sheets, and their thicknesses could be controlled by the layer number. For instance, 20 layers of MWCNT sheets had produced a thickness of around 450 nm which was mainly investigated in this work. Therefore, the average thickness of a layer of MWCNT sheet was about 23 nm. Polymer solutions were then coated onto the MWCNT sheet to produce an aligned MWCNT/polymer composite film. Polymers were located at the voids among MWCNTs. Here, poly (methyl methacrylate) (PMMA) was used as a model as it had been widely investigated. After incorporation of PMMA, the resulting composite film retained the original size of the pure MWCNT sheet, and the aligned structure of MWCNTs had been also well maintained (Fig. 2c and d). The atomic force microscopy (AFM) image (Fig. 2d) further showed that the side walls of MWCNTs were exposed on the film surface. To further investigate the surface morphology of the composite film, we had scanned the film surface by AFM and obtained the height graph. Obviously, the side walls of MWCNTs were exposed to the surface of composite film, and PMMA was infiltrated among the MWCNTs to stabilize them. Of course, other polymers such as epoxy resin had been also used to produce the similar structure, and the cross-sectional SEM (Fig. S3) further confirmed the aligned structure of MWCNTs in such composite materials. The tribological properties of MWCNT/PMMA composite materials were mainly studied in the following discussion.

AFM had been proposed as an efficient tool to investigate the micro-friction behavior of nanomaterials [31–36]. As shown in Fig. S4, a modified cantilever with a silica bead at the end was used as the AFM tip [34]. Fig. S5 showed the friction signal (reflected by the output voltage) during a typical scanning cycle under an external load range between 0 and 100 nN. The output voltages were obviously varied in both forward and backward directions, which could be attributed to the aligned MWCNTs at the tested surface of the composite film. To be accurate, the friction signal mentioned below was calculated as an average result of 256 scanning cycles for each sample.

Fig. 3 had compared the friction signals with the increasing external load from 0 to 100 nN in both longitudinal and transverse directions relative to the MWCNT length. It can be seen that the output voltage was linearly increased with the increasing external load in both directions. However, the slopes in two directions were different. As the friction signal was directly related to the real friction force, the slope of the fitted line can reflect the friction coefficient of the composite film [37]. Herein, we had summarized the friction coefficients of 25 samples in two directions (Fig. S6). It was found that the average friction coefficient in the longitudinal direction was calculated to be 0.0343, compared with 0.0692 in the transverse direction (Fig. 4). Obviously, the composite film showed an anisotropic behavior in the micro-tribological property with the ratio of friction coefficients between transverse and longitudinal directions being about 2 [10,35,38]. As a control, we had also prepared randomly dispersed MWCNT/PMMA composite films and compared the micro-friction behavior in different directions (Fig. S7). It was found that the friction coefficients were maintained to be close in all directions (Fig. S8).

The aligned MWCNT/PMMA composite films also exhibited excellent electrical, mechanical, and thermal properties, which
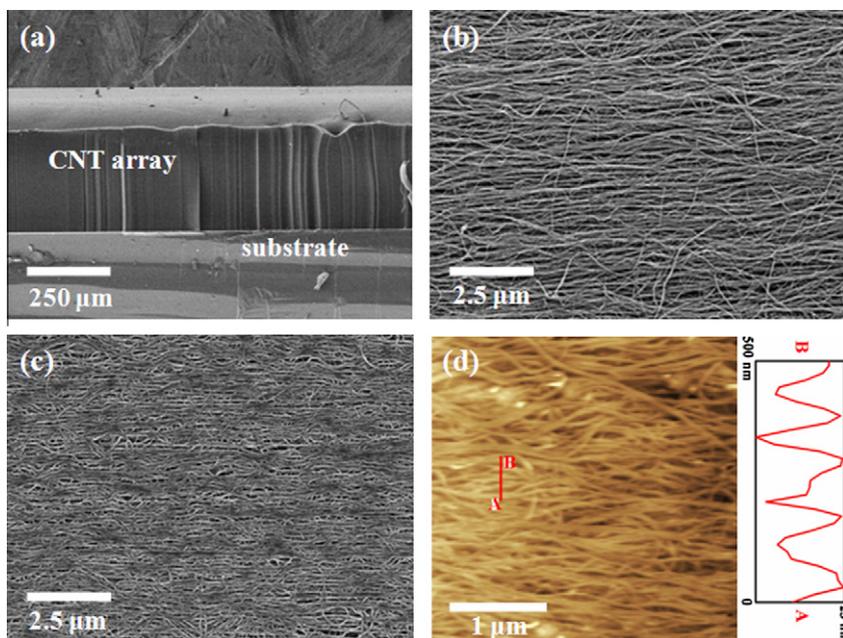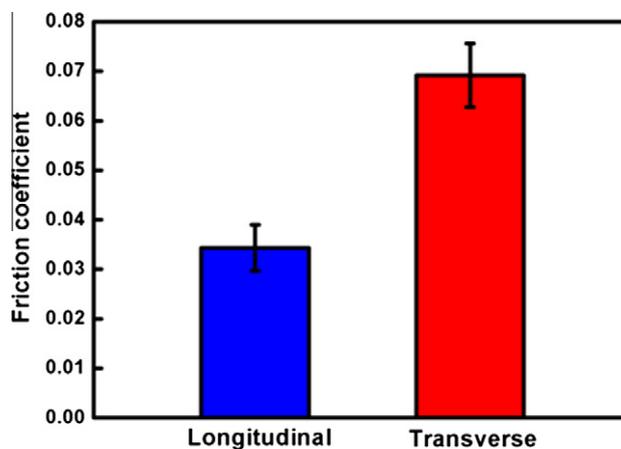
Fig. 2. Scanning electron microscopy (SEM) and atomic force microscopy (AFM) characterizations. (a) SEM image of an MWCNT array. (b) SEM image of a pure MWCNT sheet. (c) SEM image of an aligned MWCNT/PMMA composite films from a top view. (d) AFM image of the surface of an aligned MWCNT/PMMA composite films.
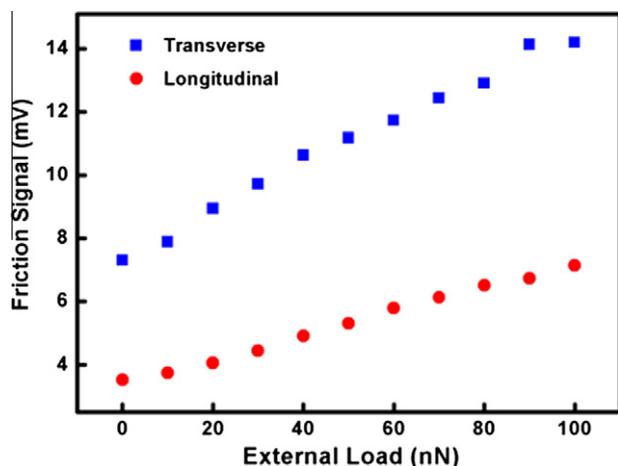
Fig. 3. Dependence of the friction signal on external load in the transverse (blue color) and longitudinal (red color) directions relative to the MWCNT length.

Fig. 4. Summary of the friction coefficients in the longitudinal and transverse directions relative to the MWCNT length. The data for each direction were obtained from 25 samples.

were critically important for the use as high-performance friction materials [39,40]. In particular, the composite film was anisotropic in electrical conductivity, for example, about 10^2 S/cm along the MWCNT length and 10^1 S/cm in the perpendicular direction relative to the MWCNT length (Fig. S9). The electrically conductive property can effectively prevent the charge accumulation in the composite material [24]. The aligned MWCNT/PMMA film also showed an anisotropic mechanical property, for example, a tensile strength of 88 MPa along the MWCNT length and 14 MPa in the perpendicular direction relative to the MWCNT length (Fig. S10a and b). It should be noted that a randomly dispersed MWCNT/PMMA film had a tensile strength of 44 MPa (Fig. S10c). In addition, the composite film indicated a much improved thermal stability after incorporation of MWCNTs. For instance, the decomposition temperature of the composite film can be improved by about 10 °C compared with the pure PMMA (Fig. S11). Here, the decom-

position was composed of two steps, that is, decomposition of PMMA between 300 and 400 °C and MWCNTs at ~700 °C.

4. Conclusion

In summary, we had developed a general method to prepare highly aligned MWCNT/polymer films in which parts of the MWCNT side walls were embedded in the polymer matrix, while the others were exposed in the air on the surface. These composite films represented the first material which showed an anisotropic tribological property. The friction coefficient in the transverse direction was about 2 times of that of longitudinal direction. In addition, the aligned MWCNTs provided the composite film with excellent electrical, mechanical, and thermal properties. This work also presented an efficient paradigm to synthesize high-performance friction materials with an anisotropic tribological behavior by introduction of one-dimensional nanostructures.

Acknowledgments

Appendix A. Supplementary material

Supplementary material associated with this article can be found, in the online version, at http://dx.doi.org/10.1016/j.jcis.2012.12.024.

References

[1] N.K. Myshkin, M.I. Petrokovets, A.V. Kovalev, Tribol. Int. 38 (2005) 910.
[2] S.K. Sinha, C.B. Lee, S.C. Lim, Tribol. Lett. 29 (2008) 193.
[3] M.A. Samad, N. Satyanarayana, S.K. Sinha, Surf. Coat. Technol. 204 (2010) 1330.
[4] L. Lin, D. Kim, Tribol. Int. 2011 (1926) 44.
[5] L. Sun, Z. Yang, X. Li, Wear 264 (2008) 693.
[6] T. Larsen, T.L. Andersen, B. Thorning, M.E. Vigild, Wear 264 (2008) 857.
[7] G. Pan, Q. Guo, J. Ding, W. Zhang, X. Wang, Tribol. Int. 43 (2010) 1318.
[8] K.S. Kim, Y. Ando, K.W. Kim, Nanotechnology 19 (2008) 105701.
[9] P. Samyn, G. Schoukens, P. De Baets, Appl. Surf. Sci. 256 (2010) 3394.
[10] R.W. Carpick, D.Y. Sasaki, A.R. Burns, Tribol. Lett. 7 (1999) 79–85.
[11] P.L. Dickrell, S.B. Sinnott, D.W. Hahn, N.R. Raravikar, L.S. Schadler, P.M. Ajayan, W.G. Sawyer, Tribol. Lett. 18 (2005) 59.
[12] M. Yang, W. Wang, I. Lieberwirth, G. Wegnar, J. Am. Chem. Soc. 131 (2009) 6283.
[13] M.A. Correa-Duarte, L.M. Liz-Marzán, J. Mater. Chem. 16 (2006) 22.
[14] Y. Xiang, X. Wu, D. Liu, Z. Li, W. Chu, L. Feng, K. Zhang, W. Zhou, S. Xie, Langmuir 24 (2008) 3465.
[15] P.H. Yeh, Z. Li, Z.L. Wang, Adv. Mater. 21 (2009) 4975–4978.
[16] S. Hong, S. Myung, Nat. Nanotechnol. 2 (2007) 207.
[17] M.F. Yu, B.S. Files, S. Arepalli, R.S. Ruoff, Phys. Rev. Lett. 84 (2007) 5552.
[18] B.G. Demczyk, Y.M. Wang, J. Cumings, M. Hetman, W. Han, A. Zettl, R.O. Ritchie, Mater. Sci. Eng. A 334 (2002) 173.
[19] S. Berber, Y.K. Kwon, D. Tománek, Phys. Rev. Lett. 84 (2000) 4613.
[20] H. Peng, X. Sun, F. Cai, X. Chen, Y. Zhu, G. Liao, D. Chen, Q. Li, Y. Lu, Y. Zhu, Q. Jia, Nat. Nanotechnol. 4 (2009) 738.
[21] D. Shi, Adv. Funct. Mater. 19 (2009) 3356.
[22] H.J. Jeong, H.D. Jeong, H.Y. Kim, J.S. Kim, S.Y. Jeong, J.T. Han, D.S. Bang, G.W. Lee, Adv. Funct. Mater. 21 (2011) 1526.
[23] A. Zloczewska, M. Jonsson-Niedziolka, J. Rogalski, M. Opallo, Electrochim. Acta 56 (2011) 3947.
[24] M. Moniruzzaman, K.I. Winey, Macromolecules 39 (2006) 5194–5205.
[25] F. Du, R.C. Scogna, W. Zhou, S. Brand, J.E. Fischer, K.I. Winey, Macromolecules 37 (2004) 9048.
[26] L. Li, Z. Yang, H. Gao, H. Zhang, J. Ren, X. Sun, T. Chen, H.G. Kia, H. Peng, Adv. Mater. 23 (2011) 3730.
[27] T. Chen, Z. Cai, Z. Yang, L. Li, X. Sun, T. Huang, A. Yu, H.G. Kia, H. Peng, Adv. Mater. 23 (2011) 4620.
[28] W. Guo, C. Liu, X. Sun, Z. Yang, H.G. Kia, H. Peng, J. Mater. Chem. 22 (2012) 903.
[29] Z. Yang, X. Sun, X. Chen, Z. Yang, G. Xu, R. He, Z. An, Q. Li, H. Peng, J. Mater. Chem. 21 (2011) 13772.
[30] H. Peng, J. Menka, D.E. Peterson, Y. Zhu, Q. Jia, Small 2008 (1964) 4.
[31] J.P. Tu, L.P. Zhu, K. Hou, S.Y. Guo, Carbon 41 (2003) 1257.
[32] H. Kinoshita, I. Kume, M. Tagawa, N. Ohmae, Appl. Phys. Lett. 85 (2004) 2780.
[33] H. Lu, J. Goldman, F. Ding, Y. Sun, M.X. Pulikkathara, V.N. Khabashesku, B.I. Yakobson, J. Lou, Carbon 46 (2008) 1294.
[34] J. Lou, K.S. Kim, Mater. Sci. Eng. A 483–484 (2008) 664.
[35] M. Lucas, X. Zhang, I. Palaci, C. Klinke, E. Tosatti, E. Riedo, Nat. Mater. 8 (2009) 876.
[36] J. Ou, J. Wang, S. Liu, B. Mu, J. Ren, H. Wang, S. Yang, Langmuir 26 (2010) 15830.
[37] X.C. Lu, B. Shi, L.K.Y. Li, J. Luo, J. Wang, H. Li, Surf. Coat. Technol. 128–129 (2000) 341.
[38] Y. Inoue, Y. Suzuki, Y. Minami, J. Muramatsu, Y. Shimamura, K. Suzuki, A. Ghemes, M. Okada, S. Sakakibara, H. Mimura, K. Naito, Carbon 49 (2011) 2437.
[39] A. Benedetto, P. Viel, S. Noël, N. Izard, P. Chenevier, S. Palacin, Surf. Sci. 601 (2007) 3687.
[40] M.A. Samad, S.K. Sinha, Tribol. Int. 2011 (1932) 44.